IEEE Access
Multidisciplinary : Rapid Review : Open Access Journal

Received 23 September 2023, accepted 14 October 2023, date of publication 23 October 2023, date of current version 2 November 2023.

Digital Object Identifier 10.1109/ACCESS.2023.3327179

RESEARCH ARTICLE

Determination of the Plasma Density in a Plasma Antenna Based on Image Analysis and LIVPD Graphs

MOHAMMAD-REZA DORBIN[1], JALIL A. RASHED MOHASSEL[1], (Life Senior Member, IEEE), FATEMEH SADEGHIKIA[2], AND HAJAR BINTI JA'AFAR[3], (Member, IEEE)

[1]School of ECE, College of Engineering, University of Tehran, Tehran 1439957131, Iran
[2]Wireless Telecommunication Group, ARI, Ministry of Science, Research and Technology, Tehran 1465774111, Iran
[3]School of Electrical Engineering, College of Engineering, Universiti Teknologi MARA, Shah Alam 40450, Malaysia

Corresponding author: Fatemeh Sadeghikia (sadeghi_kia@ari.ac.ir)

ABSTRACT This paper introduces an innovative method for quantitatively determining plasma density in plasma columns, with particular applicability to reconfigurable antennas. This method significantly enhances the speed of capturing density variations, particularly in surface wave-excited antennas. By utilizing images of excited plasma tubes, the proposed approach extracts a light intensity versus plasma density (LIVPD) graph, creating a direct correspondence between visible light intensity and plasma density. The methodology, encompassing LIVPD graph extraction and plasma density evaluation, is comprehensively elucidated. Rigorous analytical and experimental validations confirm a minor deviation of approximately 8.5%. The versatility of the method is demonstrated through two practical applications, reaffirming its accuracy in challenging scenarios. Additionally, this study includes a comparative analysis that highlights the superiority of the method in terms of sampling rate, measurement points, and non-intrusiveness over conventional techniques. This paper thus presents a robust method with promising potential for accurate plasma density determination in diverse antenna applications.

INDEX TERMS Plasma antenna, image processing technique, plasma density, determination of the plasma density, surface wave.

I. INTRODUCTION

In recent years, reconfigurable antennas have garnered significant attention for their ability to achieve diverse radiation patterns and operating frequencies, thereby reducing the complexity of communication systems. Various techniques, including electrical, optical and material based mechanisms, have been explored for implementing reconfigurable antennas [1], [2]. Among these techniques, the utilization of tunable materials like liquid metals and plasmas has arisen as a promising direction [3], [4], [5]. Plasma, as the fourth state of matter, offers unique properties that have stimulate numerous studies on reconfigurable plasma antennas [6], [7], [8], [9], [10]. These antennas leverage the reconfigurability of radiation characteristics and tunable resonant frequencies afforded by plasma.

Plasma density measurement is crucial for understanding the behavior of plasma antennas and reconfigurable systems [7]. Conventional methods, such as phase difference detection [7], spectroscopy [11], Langmuir probes [12], waveguide cutoff frequency analysis [13], current probe [14], and microwave interferometry [12], [15], have been widely used for this purpose. However, these methods often encounter limitations in various scenarios, including cases where rapid plasma density variations occur during excitation in a millisecond range [16], [17] or when the presence of probes or instruments interferes with wave propagation, particularly when surface wave (SW) excitation is employed [18].

In response to these challenges, a pioneering method has emerged as an efficacious tool for plasma density measurement, particularly in SW-excited plasmas. This innovative approach supports nearly fast variations in plasma density, avoiding the need for intrusive probes. At its core, the method entails the extraction of a graph establishing a direct correlation between plasma density and the visible light intensity emanating from the plasma tube. Remarkably, the autonomy of this graph from the excitation method and its unique

The associate editor coordinating the review of this manuscript and approving it for publication was Chinmoy Saha.

association with specific gas types and pressure ranges for each plasma tube make it an invaluable resource. Capitalizing on this graph, the technique facilitates the determination of plasma density distribution along the plasma column by tracking fluctuations in visible light intensity. This non-intrusive imaging of the stimulated plasma column enables real-time observations of plasma behavior, while preserving the integrity of the plasma itself.

To uncover the potential of this new method, the paper is organized in a structured manner. The initial part focuses on the methodology developed for assessing plasma density within a plasma column. This section encompasses guidelines for extracting the LIVPD graph. Subsequent stages involve the determination of plasma density based on this graph and the subsequent validation process. Moving forward, two tangible applications of the proposed technique are introduced in the following section, highlighting its practical utility. Furthermore, a comparative analysis between conventional plasma density measurement techniques and our innovative approach, centered around the LIVPD graph, is provided. The study will be concluded and summarized in the final section.

II. METHODOLOGY

This section presents the devised methodology for evaluating plasma density within a plasma column. The process consists of three core steps: 1) Extracting the LIVPD graph for a specific plasma tube, 2) Estimating the plasma density for the plasma tube using the extracted LIVPD graph under different physical parameters and excitations, and 3) validation of the method. The section begins by introducing the LIVPD graph concept and detailing the process of graph extraction from a commercial fluorescent lamp. Subsequently, leveraging the extracted LIVPD graph, the distribution of plasma density along the lamp is determined under diverse excitation conditions. Demonstrating the reliability of the method concludes this section.

A. THE LIVPD GRAPH: DESCRIPTION AND EXTRACTION

This subsection underscores the foundational role of the LIVPD graph in plasma density estimation. The graph portrays the correlation between visible light intensity and plasma density within a designated plasma tube. It is elaborated how the LIVPD graph is introduced and described, and the technique for extracting this graph from a commercial fluorescent lamp is elucidated.

Within a plasma tube, the observable light intensity is influenced by various plasma attributes, including plasma density, gas composition, tube material, configuration, and fluorescent coatings [19], [20]. However, directly deriving light intensity from these parameters presents a complex challenge. Notably, in scenarios where gas composition and parameters remain constant, light intensity closely associates with plasma density or electron temperature, implying that higher light intensity corresponds to higher plasma density.

To extract the LIVPD graph for a plasma tube, a controllable excitation circuit for exciting the plasma tube is necessary which similar to DC excitation, provides a nearly constant density over the time in the column. Variations of the excitation power changes the light intensity in the tube. To capture images of the plasma tube under varying excitation powers, it is essential to use a camera with a higher shutter speed and lower ISO value to avoid picture saturation. In this investigation, the shutter speed and ISO value of camera are respectively 1 ms and 50. To normalize the light intensity in the picture, a reference intensity from a LED lamp is used. At each excitation power, the plasma density of the tube is measured. Mapping the light intensity and plasma density in different excitation powers produces a data source which is known in this investigation as the LIVPD graph.

In this section, a microwave cavity is used for the measurement of the plasma density to extract LIVPD graph. This method was previously discussed in [21] for measuring plasma density within a cylindrical DC-excited plasma column. The schematic in Fig. 1(a) illustrates the resonant microwave cavity deployed for evaluating plasma permittivity in a cylindrical plasma tube. This setup incorporates ports for excitation and measurement, along with apertures for inserting the plasma tube. These ports specifically serve as input and output interfaces for the electromagnetic waves propagating within the cavity.

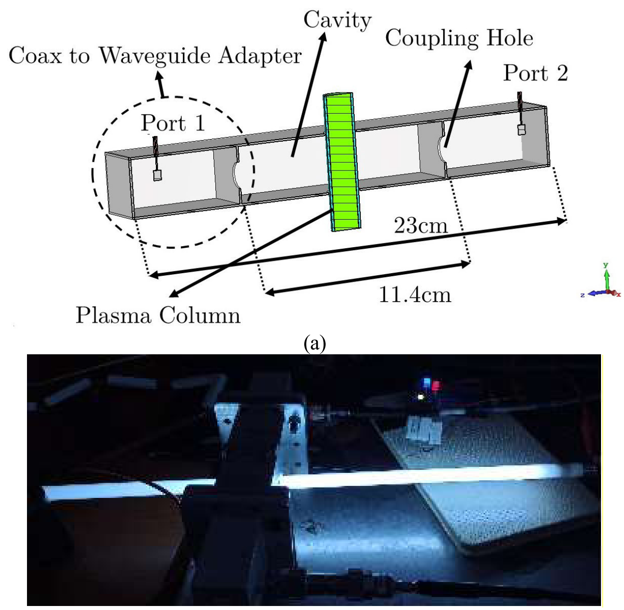

(a)

(b)

FIGURE 1. (a) The structure of a microwave cavity that measures the permittivity of the plasma in a tube. (b) An illustration of the measurement procedure.

A commercial fluorescent lamp, 28 cm long with an 8 mm radius, is examined as a case study. Fig. 1(b) illustrates the measurement process for the DC-excited lamp, with excitation power governed by a variable resistor in the excitation circuit. The method starts by exciting the resonant cavity and assessing its S_{21} parameter using a network analyzer. Extracting the resonant frequency and Q factor facilitates electromagnetic field calculations within the cavity using the stationary method and consequently, the plasma and collision frequencies are extracted within the lamp [21]. Fig. 2 displays measured S_{21} parameters for the lamp across various excitation powers, showcasing the anticipated rise in resonant frequency with increased excitation power.

Finally, with knowledge of the plasma frequency and collision frequency, the plasma density (n) of the plasma column can be determined using the following equation:

$$\omega_p = (ne^2)/(\varepsilon_0 m_e), \tag{1}$$

where e is the electron charge, m_e is the electron mass, and ε_0 is the permittivity of free space. The estimated collision frequency for the fluorescent lamp in this investigation is around $\upsilon = 2$ GHz.

Fig. 3 illustrates the LIVPD graph, with relative light intensity on the horizontal axis and plasma density on the vertical axis. This graph serves as a foundation for estimating plasma density distribution under varying excitation sources.

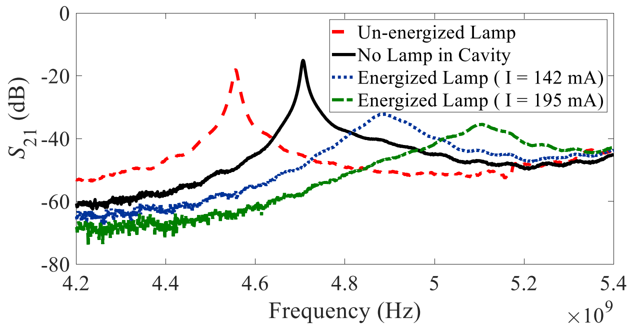

FIGURE 2. The measured S_{21} of the DC-excited fluorescent lamp inserted in the microwave cavity.

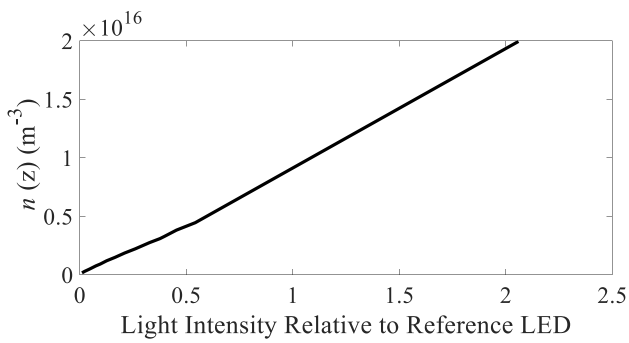

FIGURE 3. The extracted LIVPD graph of the fluorescent lamp.

B. DETERMINATION OF THE PLASMA DENSITY BASED ON THE LIVPD GRAPH

This segment focuses on estimating plasma density distribution along the fluorescent lamp, leveraging the previously extracted LIVPD graph. This determination is made for a SW-excited lamp.

SW excitation involves applying radio frequency (RF) electromagnetic waves to propagate along the plasma boundary. The SW launcher includes a 30 mm copper collar positioned 2 mm below from the top surface of a grounded box. By utilizing 6 MHz RF power, the ionized plasma column extends around 17 cm within the lamp, indicating that the ionized plasma doesn't entirely fill the 28 cm length. Plasma density distribution is determined by analyzing lamp images in correlation with the LIVPD graph from Figure 3. Using interpolation on this graph, the resulting plasma density distribution is illustrated in Figure 4 with a solid black line.

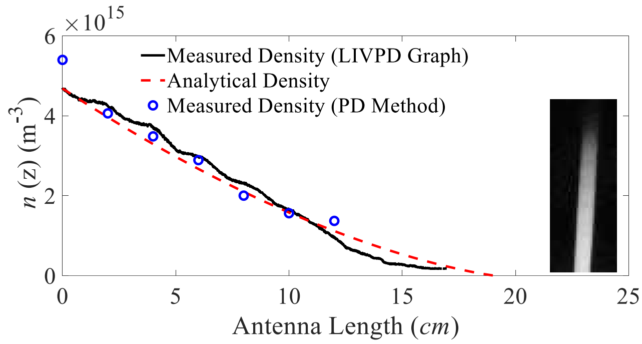

FIGURE 4. Distribution of the plasma density along the SW excited plasma column by LIVPD graph, analytical technique, and experimental method.

C. VALIDATION OF THE METHOD

The validation of the proposed plasma density distribution involves two methods: analytical validation and a previously established experimental method based on phase difference detection using a microchip.

For the analytical validation, a well-accepted and commonly known approximation for the distribution of the plasma density along a SW excited plasma column is used here which belongs to the cases that the plasma column has not reached the far end of the tube and is expressed as:

$$n(z) \approx n_d + C\upsilon\,(h - z) \tag{2}$$

in which h is the height of the plasma column, C is a constant that depends on the tube geometry and is investigated in detail in [7], z is the distance from the excitation point, and n_d is the plasma density at the end of the plasma tube and is given by:

$$n_d = \frac{\varepsilon_0 m_e}{e^2}\omega_{exc}^2\left(1 + \varepsilon_g\right) \tag{3}$$

in which ε_g is the relative permittivity of the tube, and ω_{exc} is the angular frequency of the RF excitation wave. Considering equations (2) and (3), the distribution of the plasma density along the column is analytically calculated and the result is illustrated by the dashed red line in Fig. 4. Comparison between the calculated distribution and the estimated density from the LIVPD graph reveals an approximately 9.3 % discrepancy between the results, as tabulated in Table 1. The relative errors (in percent) are obtained as (experimental density using LIVPD – analytical density) / experimental density using LIVPD × 100.

For experimental validation, plasma density distribution is estimated based on phase difference (PD) measurements along the column using a phase difference detector microchip, as introduced by the authors in [6]. The resulting

TABLE 1. Comparison between plasma density values extracted by different methods: analytical, experimental based on LIVPD graph and experimental based on phase difference (PD) measurements.

Distance (cm)	Analytical Density ($\times 10^{15}$ cm^{-3})	Experimental density ($\times 10^{15}$ cm^{-3})		Relative Error (%)	
		PD	LIVPD	Between Analytical & LIVPD	Between PD & LIVPD
2	3.96	4.059	4.24	6.6	4.2
4	3.29	3.48	3.66	10.1	4.9
6	2.67	2.89	2.98	10.4	3.0
8	2.09	2.00	2.31	9.5	13.4
10	1.58	1.56	1.64	3.6	4.8
12	1.11	1.37	0.96	15.6	42.7

measurements align with the LIVPD graph-derived estimates, with an average discrepancy of around 12.2%, as shown in detail in table 2.

Given the discrepancies within acceptable limits, the proposed methodology is validated for applications, particularly where other practical or analytical tools are lacking. This comprehensive approach establishes an efficient means to characterize plasma density distribution in plasma antennas, enhancing understanding of their performance under diverse excitation conditions.

III. APPLICATIONS OF THE METHOD

This section unveils the compelling applications of the proposed plasma density determination method within a plasma column. The technique proves highly effective in investigating the physical parameters of plasma antennas. Particularly, in SW-excited plasma antennas, scenarios arise where the excitation power is so intense that the plasma column reaches the end of the tube, thereby rendering theoretical predictions of plasma distribution impractical. Additionally, proximity to measurement instruments can perturb SW propagating paths. In this context, the presented method offers a viable solution. The subsequent subsections illustrate two distinct applications to underscore the versatility of the method.

A. FIRST CASE

As a primary application, the method is applied to a commercial fluorescent lamp, as described in Section II. The lamp is excited by a surface wave at 6 MHz, with an excitation power sufficient to fill the tube. By utilizing the LIVPD graph extracted in Section II (illustrated in Fig. 3) and analyzing captured images of the lamp, the plasma density is estimated, as presented in Fig. 5. The results indicate a linear reduction in plasma density from the excitation point to the end of the tube. Notably, the density at the end of the tube remains relatively constant, regardless of excitation power. Thus, at the investigated frequency of 6 MHz, which is recognized as low within the scope of this study, the plasma density gradually diminishes along a fully ionized tube, progressively decreasing from the excitation point to the far end of the column.

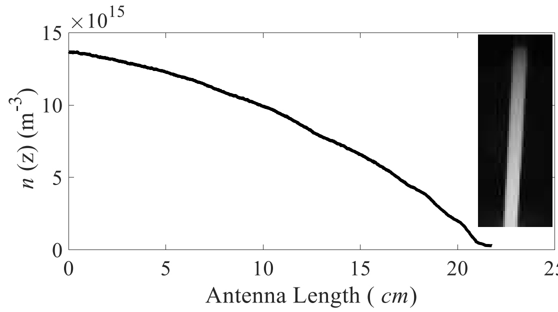

FIGURE 5. Distribution of the plasma density along the fully ionized SW excited fluorescent lamp at the excitation frequency of 6 MHz extracted by LIVPD graph.

B. SECOND CASE

The second application exemplifies the versatility of the method by applying it to a commercial Neon lamp. This lamp features a length of 1.2 m, a radius of 6 mm, and operates at a gas pressure of 500 mTorr. This scenario serves to demonstrate the efficacy of the method under different conditions. Employing SW excitation, a 600 W commercial magnetron is employed to excite the lamp at a frequency of 2.4 GHz. It's important to note that the excitation frequency in this case is significantly higher than the previous example of 6 MHz.

To facilitate this excitation, the lamp is placed within a wooden structure, as depicted in Fig. 6(a). The upper surface of the structure, functioning as the ground plane for the plasma column, is coated with a thin copper layer. By manipulating the distance between the lamp and the magnetron antenna using a wooden slab, the power level of the excitation can be controlled. Fig. 6(b) and 6(c) show visual representations of the lamp at different excitation powers.

Nevertheless, using a commercial magnetron presents a challenge due to its inconsistent output power. Through slow-motion video recording, it is observed that the height of the plasma column undergoes periodic oscillations at a frequency of 50 Hz. This implies a 20 ms cycle for variations in plasma density within the column. To ensure that plasma density distribution remains constant during measurement, observations need to be conducted within a timeframe shorter

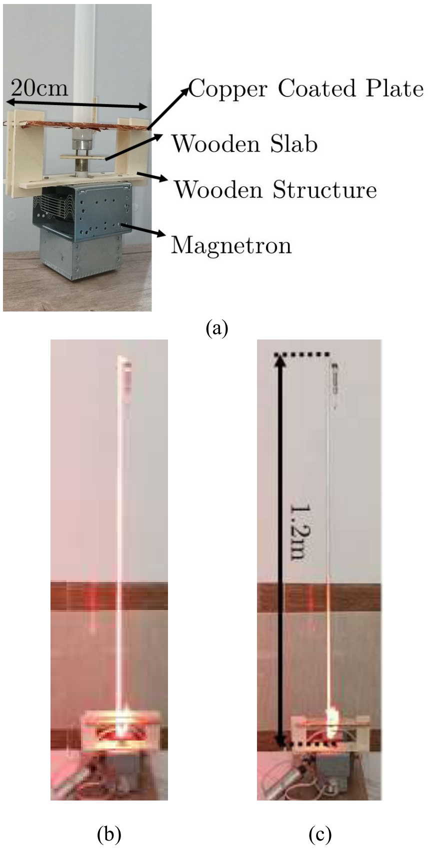

FIGURE 6. (a) The structure of a magnetron wave launcher, (b) full-length excited Neon lamp, (c) partially excited Neon lamp.

than one-tenth of a full period of plasma density variation, approximately 2 ms for this study. This ensures the stability of plasma density measurements.

Initially, it's essential to extract the LIVPD graph for this lamp. This is achieved by employing a camera with a shutter speed of 0.25 ms and a dark lens to prevent image saturation. The excited plasma within the lamp covers a length of 98 cm during this procedure, indicating that the lamp is not fully saturated with plasma. Analytical estimation of the plasma density distribution along the column at different points of the tube becomes feasible using equations (2) and (3) in such cases. The resulting LIVPD graph is illustrated in Figure 7.

Subsequently, the utility of this graph comes to the forefront, particularly in cases where theoretical formulations for plasma density estimation are absent. This scenario occurs when the tube is completely filled with plasma. By inserting a thin conducting plate perpendicular to the lamp axis and positioned 14 cm away from the excitation box (as shown in Fig. 8(a)), the propagation of SWs beyond the plate is prevented. Consequently, a fully excited plasma column with a height of 14 cm is achieved, as depicted in Fig. 8(b). Utilizing the extracted LIVPD graph for this lamp, the distribution of plasma density along the ionized region is calculated and presented in Fig. 8(c). This graph highlights the non-linear distribution of plasma density within the excited region of the tube, attributed to the reflection of SWs from the conducting plate, leading to the formation of standing wave patterns.

In summary, the proposed method adeptly determines the distribution of plasma density within plasma antennas. The scenarios showcased in this section yield insights that the distribution of plasma density within a fully ionized tube is intrinsically tied to the excitation frequency. Particularly, at lower excitation frequencies (e.g., around 6 MHz), the distribution of plasma follows an almost linear pattern. However, at higher excitation frequencies (around 2.4 GHz and beyond), the plasma density assumes a sinusoidal pattern and is no longer linear along the excited length. These observed behaviors will be further discussed in future publications.

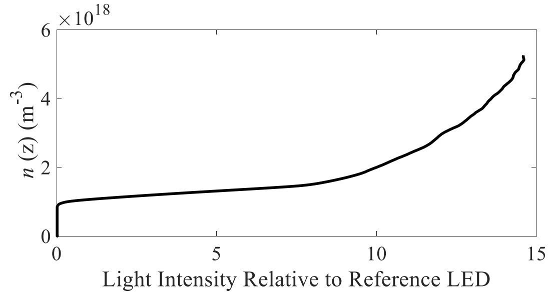

FIGURE 7. The LIVPD graph of the Neon lamp.

IV. COMPARATIVE ANALYSIS OF PLASMA DENSITY MEASUREMENT TECHNIQUES

This section presents a comprehensive comparative analysis of conventional plasma density measurement techniques alongside our newly developed LIVPD graph-based approach. The assessment focuses on critical parameters, including sampling rate, number of measurement points, and the proximity of obstacles to the plasma, as summarized in Table 1.

The comparative evaluation highlights the distinct advantages of our innovative LIVPD graph method in comparison to conventional techniques. This approach demonstrates a moderate to high sampling rate, which is indicative of the frequency at which measurements are acquired, a significantly greater number of measurement points per sample, and non-intrusive measurement capabilities. Sampling rate classifications are categorized as L: Low (sampling rate < 2 Hz), M: Moderate (2 Hz $<$ sampling rate $<$ 2 kHz), and H: High (sampling rate $>$ 2 kHz). These attributes collectively position it as an invaluable tool for precise and pragmatic plasma density determination across diverse antenna applications. However, the main disadvantage of this method is the necessitate of extracting the LIVPD graph for each plasma tube distinctly.

This comparative analysis substantiates superiority of the LIVPD graph method, marked by its adaptability to different sampling rates, abundant measurement points, and non-interfering nature. As contemporary plasma antenna research seeks enhanced precision and practicality, the LIVPD graph method emerges as an instrumental advancement in plasma density measurement techniques.

The primary limitation of this approach is the requirement to extract a distinct LIVPD graph for each individual plasma tube before conducting measurements. Notably, this method

TABLE 2. Comparison between plasma density measurement techniques.

Method	Sampling Rate Classification	Number of Points in One Measure	Obstacle Presence Near Plasma
Langmuir probe	L	1	Yes
Wave cut off method	L	1	Yes
Microwave interferometer	H	1	No
Phase difference method	H	1	Yes
Optical emission spectroscopy	M	1	Yes
Current probe	H	1	Yes
Cavity method	L	1	Yes
LIVPD graph method	M to H	Related to picture resolution ~1000	No

L: Ssampling Rate < 2 Hz, M: 2 Hz < Sampling Rate < 2 KHz, and H: Sampling Rate > 2 KHz.

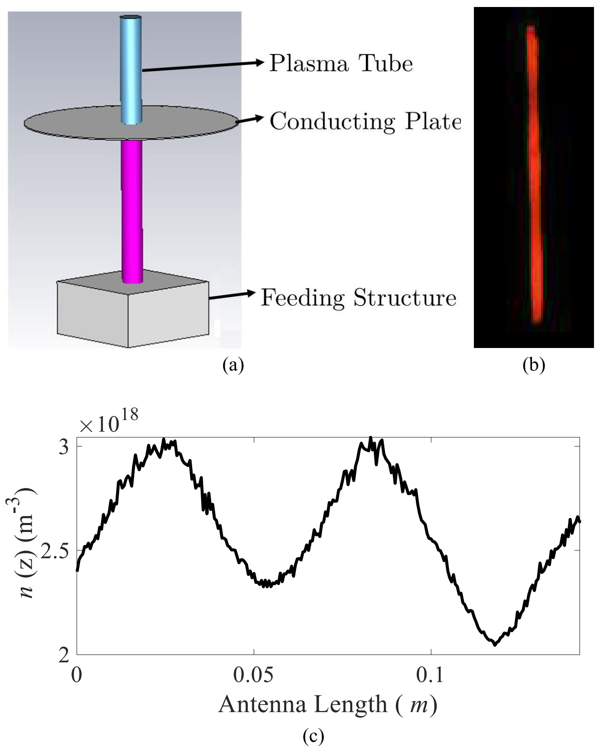

FIGURE 8. (a) Schematic of the 1.2 m Neon lamp excited by surface waves (SW), illustrating the insertion of a conducting plate 14 cm from the excitation point, perpendicular to the tube axis. (b) Photograph of the lamp displaying the ionized plasma region. (c) Distribution of plasma density along the excited section, computed using the LIVPD graph.

is specifically applicable to transparent plasma tubes where visible light is present within the plasma column. Additionally, the achievable sampling rate classification is heavily reliant on the inherent capabilities of the camera employed. Enhanced cameras permit higher sampling rates within this method.

V. CONCLUSION

In conclusion, this paper introduces a pioneering technique for accurately determining plasma density along a plasma column, with specific emphasis on reconfigurable plasma antennas. The proposed method capitalizes on image analysis and the LIVPD graph to estimate plasma density distribution. The adaptability of the method to different sampling rates, extensive measurement points in single measurement, and non-intrusive nature make it a valuable advancement. It overcomes challenges posed by fast plasma density variations and obtrusive probes. The efficacy of the method is validated both analytically and experimentally. The presented applications demonstrate its potential to unveil the intricate relationship between plasma density and excitation frequency, paving the way for advancements in reconfigurable antenna technology. The comparative analysis underscores the clear advantages and drawbacks of this approach over traditional plasma density measurement techniques. As a future perspective, further investigations into the nonlinear behavior of plasma density under different excitation frequencies are anticipated, potentially enriching our understanding of plasma antenna performance.

ACKNOWLEDGMENT

The authors would like to thank the contributing researchers of the Wireless Telecommunication Group, ARI, the Ministry of Science, Research and Technology, Tehran, Iran, and the Antenna Research Center, School of Electrical Engineering, College of Engineering, Universiti Teknologi MARA, Cawangan Terengganu. This research was partially funded by UiTM through the International grant (No:100-TNCPI/INT 16/6/2 (078/2022)).

REFERENCES

[1] M. C. Johnson, S. L. Brunton, J. N. Kutz, and N. B. Kundtz, "Sidelobe canceling for reconfigurable holographic antenna," *IEEE Trans. Antennas Propag.*, vol. 63, no. 4, pp. 1881–1886, Apr. 2015.

[2] P. Lin, Y. Wu, Z. Wu, R. Zhuo, and J. Huangfu, "Optically switched multiband antenna based on Vivaldi structure," *Sci. Rep.*, vol. 12, no. 1, p. 15654, Sep. 2022.

[3] F. Sadeghikia, M. R. Dorbin, A. K. Horestani, M. T. Noghani, and H. Ja'afar, "Tunable inverted-F antenna using plasma technologies," *IEEE Antennas Wireless Propag. Lett.*, vol. 18, no. 4, pp. 702–706, Apr. 2019.

[4] F. Sadeghikia, A. K. Horestani, and M. Himdi, "Reconfigurable antennas based on plasma reflectors and cylindrical slotted waveguide," in *Plasma Science—Recent Advances, New Perspectives and Applications*. London, U.K.: IntechOpen, 2022. [Online]. Available: https://www.intechopen.com/online-first/84324

[5] K. Y. Alqurashi, J. R. Kelly, Z. Wang, C. Crean, R. Mittra, M. Khalily, and Y. Gao, "Liquid metal bandwidth-reconfigurable antenna," *IEEE Antennas Wireless Propag. Lett.*, vol. 19, no. 1, pp. 218–222, Jan. 2020.

[6] M.-R. Dorbin, A. K. Horestani, F. Sadeghikia, M. T. Noghani, and H. Jaafar, "Analytical study on the resonance frequency of tunable surface-wave-excited plasma antennas," *IEEE Trans. Antennas Propag.*, vol. 70, no. 10, pp. 9073–9082, Oct. 2022.

[7] M.-R. Dorbin, J. A. Rashed Mohassel, F. Sadeghikia, and H. B. Ja'afar, "Analytical estimation of the efficiency of surface-wave-excited plasma monopole antennas," *IEEE Trans. Antennas Propag.*, vol. 70, no. 4, pp. 3040–3045, Apr. 2022.

[8] M. Magarotto, L. Schenato, M. Santagiustina, A. Galtarossa, and A.-D. Capobianco, "Plasma-based reflecting and transmitting surfaces," *IEEE Access*, vol. 11, pp. 91196–91205, 2023, doi: 10.1109/ACCESS.2023.3307774.

[9] F. Sadeghikia, K. Zafari, M.-R. Dorbin, M. Himdi, and A. K. Horestani, "Reconfigurable biconcave lens antenna based on plasma technology," *Sci. Rep.*, vol. 13, no. 1, p. 9213, Jun. 2023.

[10] F. Sadeghikia, M. Talafi Noghani, and M. R. Simard, "Experimental study on the surface wave driven plasma antenna," *AEU-Int. J. Electron. Commun.*, vol. 70, no. 5, pp. 652–656, May 2016.

[11] M. Akhlaghi, H. Rajayi, A. S. Mashayekh, M. Khani, Z. M. Hassan, and B. Shokri, "On the design and characterization of a new cold atmospheric pressure plasma jet and its applications on cancer cells treatment," *Biointerphases*, vol. 10, no. 2, Jun. 2015, Art. no. 029510.

[12] G. Neumann, U. Bänziger, M. Kammeyer, and M. Lange, "Plasma-density measurements by microwave interferometry and Langmuir probes in an RF discharge," *Rev. Sci. Instrum.*, vol. 64, no. 1, pp. 19–25, Jan. 1993.

[13] J.-H. Kim, S.-C. Choi, Y.-H. Shin, and K.-H. Chung, "Wave cutoff method to measure absolute electron density in cold plasma," *Rev. Sci. Instrum.*, vol. 75, no. 8, pp. 2706–2710, Aug. 2004.

[14] P. Russo, V. M. Primiani, G. Cerri, R. De Leo, and E. Vecchioni, "Experimental characterization of a surfaguide fed plasma antenna," *IEEE Trans. Antennas Propag.*, vol. 59, no. 2, pp. 425–433, Feb. 2011.

[15] A. Daykin-Iliopoulos, F. Bosi, F. Coccaro, M. Magarotto, A. Papadimopoulos, P. De Carlo, C. Dobranszki, I. Golosnoy, and S. Gabriel, "Characterisation of a thermionic plasma source apparatus for high-density gaseous plasma antenna applications," *Plasma Sources Sci. Technol.*, vol. 29, no. 11, Nov. 2020, Art. no. 115002.

[16] P. Russo, G. Cerri, and E. Vecchioni, "Self-consistent analysis of cylindrical plasma antennas," *IEEE Trans. Antennas Propag.*, vol. 59, no. 5, pp. 1503–1511, May 2011.

[17] S. Singh, *Selected Topics in Plasma Physics*. London, U.K.: IntechOpen, Nov. 2020.

[18] M. Moisan and Z. Zakrzewski, "Plasma sources based on the propagation of electromagnetic surface waves," *J. Phys. D, Appl. Phys.*, vol. 24, no. 7, pp. 1025–1048, Jul. 1991.

[19] J. F. Waymouth and F. Bitter, "Analysis of the plasma of fluorescent lamps," *J. Appl. Phys.*, vol. 27, no. 2, pp. 122–131, Feb. 1956.

[20] P. Flesch, *Light and Light Sources*. Berlin, Germany: Springer, 2006.

[21] F. Sadeghikia, M.-R. Dorbin, J. A. R. Mohassel, and H. B. Ja'Afar, "Measurement of the plasma parameters using the stationary method in a resonant cavity," in *Proc. 17th Eur. Conf. Antennas Propag. (EuCAP)*, Mar. 2023, pp. 1–5.

MOHAMMAD-REZA DORBIN received the B.Sc. degree in electrical and electronics engineering from the Iran University of Science and Technology (IUST), in 2013, and the M.Sc. degree in electrical and electronics engineering from the University of Tehran, Iran, in 2015, where he is currently pursuing the Ph.D. degree in telecommunication engineering, with a focus on plasma antennas. His research interests include reconfigurable antennas, antenna and RCS measurement, and applications of plasma technology in wireless communications.

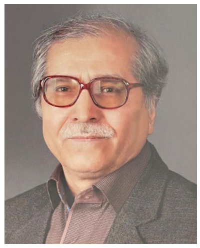

JALIL A. RASHED MOHASSEL (Life Senior Member, IEEE) received the M.Sc. degree in electronics engineering from the University of Tehran, in 1976, and the Ph.D. degree in electrical engineering from the University of Michigan, Ann Arbor, MI, USA, in 1982.

He was with the University of Sistan and Baluchestan, Zahedan, Iran, where he held several academic and administrative positions. In 1994, he joined the University of Tehran, where he is currently doing research and teaching, as a Professor of antennas, EM theory, and applied mathematics. He was the Academic Vice-Dean of the College of Engineering, the Chairperson of the School of ECE, and the General Director of educational planning and the academic affairs, University of Tehran. He was a Distinguished Professor with the First Education Festival (2008–2009), a Distinguished Pioneer Researcher, in 2020, and a Distinguished Pioneer Faculty Member with the University of Tehran, in 2022. He is a Principal Member of the Center of Excellence on Applied Electromagnetic Systems (CEAES) and the Director of the Microwave Laboratory. He is the author of three books and has published more than 220 papers in refereed journals and conference proceedings. He was a recipient of the First National "Jabehdar" Prize in Education from IEEE, Iran Section, in 2014. He served as the General Chair for the 20th ICEE, in 2012, and the second and fourth conferences on MMWaTT, in 2012 and 2016, respectively. He was a Distinguished Professor of electrical engineering with the Academy of Sciences, I.R. Iran, in 2015, a Distinguished Educator, and a Researcher with the Fourth National Communication and Information Technology Festival, Ministry of ICT, in 2014, and the IAEEE Brilliant National Researcher in the Fifth "Founder's of Science and Technology" Festival, in 2007.

FATEMEH SADEGHIKIA received the B.Sc. degree in electrical and electronics engineering from the Iran University of Science and Technology (IUST), in 2000, the M.Sc. degree in electrical and electronics engineering from the K. N. Toosi University of Technology, Iran, in 2003, and the Ph.D. degree in telecommunication engineering from IUST, in 2012, with a focus on plasma antennas. Since 2009, she has been with the Wireless Telecommunication Group, ARI, Ministry of Science, Research and Technology, Iran, where she is currently a Associate Professor. She is also directing the research and development of plasma antennas and microwave components with ARI. Her research interests include reconfigurable antennas, microwave and millimeter-wave devices, and applications of plasma technology in wireless communications. She was a recipient of the 2020 IEEE TRANSACTIONS ON ANTENNAS AND PROPAGATION Best Paper Award from the IEEE Malaysia Section.

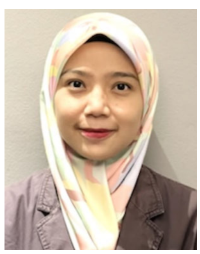

HAJAR BINTI JA'AFAR (Member, IEEE) received the Ph.D. degree in electrical engineering from Universiti Teknologi MARA, Malaysia.

She is currently a Senior Lecturer of radio frequency, microwave, and the IoT systems with Univerisiti Teknologi MARA, where she is also a Fellow Researcher with the Antenna Research Centre. She has published many publications, including high-impact journal and international conference papers. She is an Active Member of the Graduate Engineer, the Board of Engineers Malaysia (BEM), and the Institution of Engineers, Malaysia (IEM); and a member of the IEEE Antennas and Propagation Society and the Malaysia Board of Technologists (MBOT).